JOURNAL OF CATALYSIS **132,** 85–91 (1991)

A Low-Temperature IR Spectroscopic Study of Selective Adsorption of NO and CO on $CuO/\gamma\text{-}Al_2O_3$

YILU FU,[1] YANGCHAO TIAN, AND PEIYAN LIN

Department of Modern Chemistry and Structure Research Laboratory, University of Science and Technology of China, Hefei, 230026, Anhui, People's Republic of China

Received November 7, 1990; revised April 29, 1991

The composition of the crystal phase and the valence state of surface copper ions was measured by XRD and XPS methods on a $CuO/\gamma\text{-}Al_2O_3$ catalyst. It was concluded that the bulk phase was composed of CuO and $CuAl_2O_4$, and Cu^{2+} and Cu^+ ions coexisted on the surface, although the sample was oxidized in oxygen atmosphere. The infrared spectra of CO, NO, and (CO + NO) adsorbed on this catalyst were recorded from 123 to 173 K. All infrared bands were assigned. The adsorption experiment of CO and NO also demonstrated that Cu^{2+}(CuO and $CuAl_2O_4$) and Cu^+ ions coexisted on the surface. CO or NO could be adsorbed on Cu^{2+} and Cu^+ sites below 173 K, but CO was only adsorbed on Cu^+ sites and NO only on Cu^{2+} sites over 173 K. The alternate adsorption and coadsorption of NO and CO found that CO was selectively adsorbed on the Cu^+ sites (2120 cm^{-1} band) and NO was selectively adsorbed on the Cu^{2+} sites (1888 cm^{-1} on CuO and 1862 cm^{-1} on $CuAl_2O_4$), when CO and NO coexisted in the gas phase.

INTRODUCTION

Copper oxide has been used as an active component for some oxidation and hydrogenation reactions. The activity of catalytic combustion of carbon monoxide and hydrocarbons and reduction of NO_x offers an attractive means for removing these compounds from automobile exhaust. Therefore, the NO reduction by CO has received particular attention (*1–3*).

Results of CO and/or NO adsorption on copper oxides have been reported and many different surface species have been found (*3–7*). London and Bell (*3*) investigated the reaction of NO and CO on CuO/SiO_2. Based on the results of the kinetic measurements, they inferred that NO molecules were adsorbed on Cu^0 sites and Cu^+ sites were the recipients of O atoms produced in the dissociation of NO. CO was adsorbed on Cu^+ or Cu^{2+} sites. Gandhi and Shelef (*4*) studied the adsorption of NO on copper oxides. Experimental data indicated that surface cupric ions chemisorbed NO much faster than the cuprous ions. Busca (*5*) studied the CO adsorption on unreduced CuO sample using infrared spectroscopy (IR). The results showed that the IR band of CO adsorbed on Cu^+ was the strongest one. Busca believed that the surface was largely composed of a partially reduced phase (Cu_2O) although CuO is the main component in the bulk phase.

In the present paper, the phase composition of the $CuO/\gamma\text{-}Al_2O_3$ sample and the valence states were measured. The low-temperature infrared spectra of CO, NO, and (CO + NO) adsorbed on this catalyst were measured and an explicitly selective adsorption of NO and CO was observed.

EXPERIMENTAL

1. Sample Preparation

Two catalyst samples were prepared by impregnation of a calculated amount of a $Cu(NO_3)_2$ aqueous solution on $\gamma\text{-}Al_2O_3$. After the sample was dried at 373 K and decomposed at 623 K for 2 h, calcination was carried out at 1073 K for 5 h. The CuO

---

[1] To whom correspondence should be addressed.

0021-9517/91 $3.00

loading of the first sample was 5.0 wt%. Another sample that contained CuO (15.0%) was prepared for the purpose of the phase analysis.

$CuAl_2O_4$ was prepared by mixing stoichiometric amounts of $Cu(NO_3)_2 \cdot 3H_2O$ and $Al_2(SO_4)_3 \cdot 18H_2O$ in distilled water, and dried at 383 K, calcined at 1223 K for 5 h, then washed with 1 *M* $(NH_4)_2CO_3$ solution repeatedly to remove the CuO. The X-ray diffraction (XRD) pattern of the washed product only showed lines corresponding to $CuAl_2O_4$ (*8*).

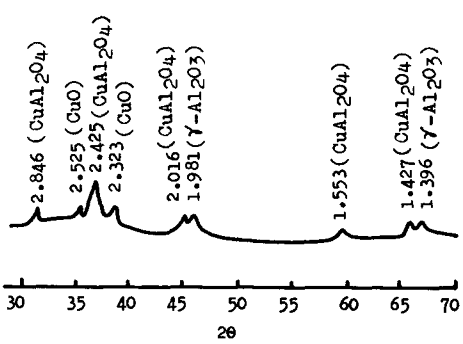

FIG. 1. The XRD spectrum of $CuO/\gamma\text{-}Al_2O_3$ (CuO 15.0 wt%).

2. *Adsorbed Gases*

The CO gas was made by the Nan Jing Analysis Instrument Factory at a nominal purity of 99.95%. It was deoxygenated by 401 deoxy agent (Hongguang Chemicals, Dalian) and dewatered by 5A zeolite. NO was prepared from the reaction of $FeSO_4$ and $NaNO_2$ in concentrated H_2SO_4. The produced gas was purified by KOH and 5A zeolite.

3. *Sample Pretreatment*

Self-supporting wafers were obtained by pressing the powder at 200 kg · cm^{-2}. They were mounted in a low-temperature IR cell (CaF_2 window), which was designed for *in situ* pretreatment and chemisorption from room temperature to 723 K and for IR measurement at low temperature from room temperature to 123 K (*13*). The sample was evacuated at 723 K for 0.5 h after treating in O_2 at 723 K for 1.5 h, then reoxidized at the same conditions and cooled down to room temperature in O_2. Finally the oxygen was pumped off.

4. *Instrumentation*

IR spectra were recorded by a Shimadzu IR-435 spectrometer, which can give differential spectra.

X-ray photoelectron spectra (XPS) were measured by an ESCA LAB MK-II instrument (VG) with a Mg*Kα* (1253.6 ev) X-ray source. Binding energies of copper were determined by reference to the C_1s peak at 284.6 ev.

XRD measurement was performed on a Model D/Max-RA diffractometer with Cu*Kα* radiation.

RESULTS

1. *Measurement of Crystal Phase*

Because of the low content and high dispersion of copper oxide, efforts to determine the crystal phases on 5.0% $CuO/\gamma\text{-}Al_2O_3$ sample were unsuccessful. For the 15.0% $CuO/\gamma\text{-}Al_2O_3$ sample, the XRD spectrum is showed in Fig. 1. It can be seen that the sample is composed of CuO and $CuAl_2O_4$ in bulk phase with copper in the +2 valence state; no other phases are detected.

2. *Measurement of Valency of Surface Copper*

The XPS of the oxidized 5.0% $CuO/\gamma\text{-}Al_2O_3$ sample is exhibited in Fig. 2. Four peaks are presented. Comparing the values of the binding energy with those in the literature, the two main peaks situated at 934.0 and 935.3 eV belong to $Cu^{2+}(2P_{3/2})$ in CuO and $CuAl_2O_4$, respectively. Besides the main peaks, the shoulder (at about 932.7 eV) belongs to $Cu^{2+}(2P_{3/2})$ (*7, 8*) and the weak peak (at 943.5 eV) is the satellite peak of Cu^{2+} (*8–12*).

The XPS of the satellite structure of Cu^{2+} compounds has been attributed to the transition of either Cu^{2+} from 3*d* to 4*s* or from

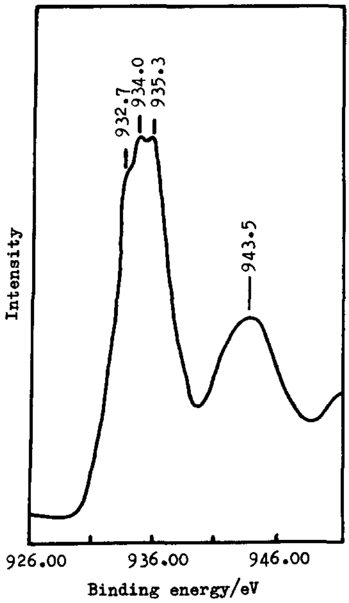

FIG. 2. The XPS of Cu($2P_{3/2}$) for CuO/γ-Al_2O_3.

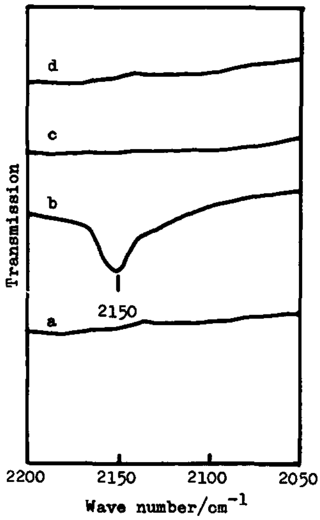

FIG. 3. IR spectra of 30-Torr CO adsorption on γ-Al_2O_3. (a) Background, (b) 123 K, (c) evacuated to 1 × 10^{-2} Torr at 123 K, (d) 173 K.

the ligand to metal (O_{2p} to Cu_{3d}). No such satellite peak is detected for Cu^+ compounds or Cu^0.

3. *Results of Low-Temperature IR Measurement*

3.1 CO adsorption. The IR spectra of 30-Torr (1 Torr = 133.3 N m^{-2}) CO adsorption on γ-Al_2O_3 at low temperature are shown in Fig. 3. One band at 2150 cm^{-1} appears at 123 K (Fig. 3b).It disappears either after evacuation at 123 K (Fig. 3c) or by raising the temperature to 173 K in CO atmosphere (Fig. 3d). This band (2150 cm^{-1}) should be assigned to the physical adsorption of CO on γ-Al_2O_3 (*13, 15*).

The IR spectra of 30-Torr CO adsorption on CuO/γ-Al_2O_3 are presented in Fig. 4. Three bands at 2170, 2148, and 2120 cm^{-1} appear at 123 K. The band at 2148 cm^{-1} is assigned to CO physical adsorption and disappears after evacuation (Fig. 4c). According to previous research (*3, 5–7*), the band at 2170 cm^{-1} is assigned to CO adsorption on Cu^{2+} and the band at 2120 cm^{-1} to CO on Cu^+ sites. After raising the temperature to 173 K in CO atmosphere (Fig. 4d), the band at 2170 cm^{-1} disappears completely while the band at 2120 cm^{-1} does not change. This means that the strength of the CO adsorption on Cu^+ sites is stronger than that on Cu^{2+} sites.

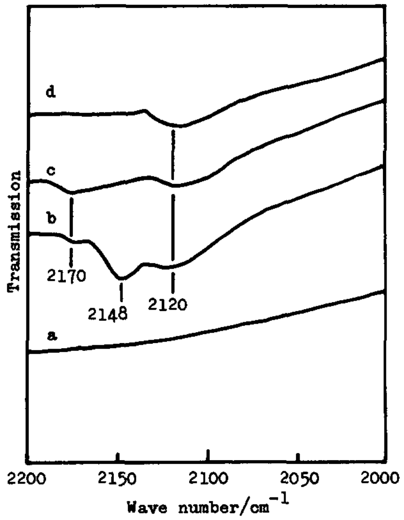

FIG. 4. IR spectra of CO adsorption on CuO/γ-Al_2O_3. (a) Background, (b) 123 K, (c) evacuated to 1 × 10^{-2} Torr at 123 K, (d) 173 K.

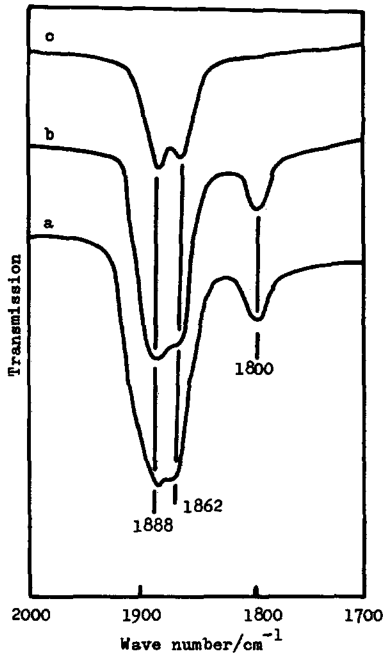

FIG. 5. IR differential spectra of NO adsorption on CuO/γ-Al_2O_3. (a) 123 K, (b) evacuated to 1 × 10^{-1} Torr at 123 K, (c) 173 K.

3.2 NO adsorption. The differential IR spectra of 25-Torr NO adsorption on CuO/γ-Al_2O_3 are shown in Fig. 5. Three bands at 1888, 1862, (shoulder), and 1800 cm^{-1} are detected at 123 K (Fig. 5a). After increasing the temperature to 173 K, the band at 1800 cm^{-1} disappears while the band at 1888 cm^{-1} still exists and the band at 1862 cm^{-1} splits from the 1888 cm^{-1} band and becomes an independent band (Fig. 5c). The band at the 1862 cm^{-1} band has never been reported. We prepared a pure $CuAl_2O_4$ compound and performed IR measurement of NO adsorption. It is found that there is only one band at 1862 cm^{-1} in this case (see Fig. 6). Thus we can assign this band to NO adsorption on another type of Cu^{2+} sites (i.e., on $CuAl_2O_4$). It is apparent that the strength of NO adsorption on Cu^{2+} sites is higher than that on Cu^{+} sites. This is the opposite of CO adsorption.

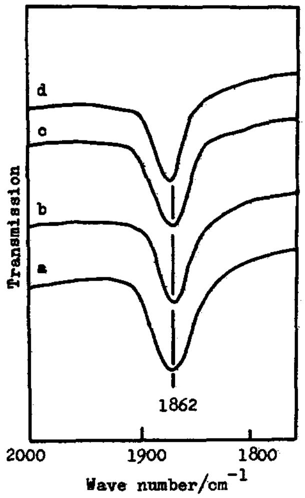

FIG. 6. IR differential spectra of NO adsorption on $CuAl_2O_4$. (a) 123 K, (b) evacuated to 1 × 10^{-1} Torr at 123 K, (c) 173 K, (d) evacuated to 1 × 10^{-1} Torr at 173 K.

3.3. Alternate adsorption of CO and NO. Alternate adsorption of CO and NO was performed in two different ways. One was preadsorption CO and then NO adsorption and the other was in inverse order.

Figure 7 exhibits the IR spectra of alternate adsorption carried out in the first way. CO (15 Torr) is preadsorbed on CuO/γ-

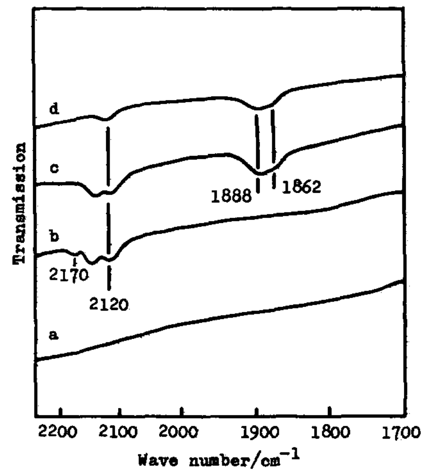

FIG. 7. IR spectra of alternate adsorption of CO and NO at 123 K. (a) Background, (b) 15-Torr CO adsorption, (c) 15 Torr NO adsorption after CO adsorption, (d) evacuated to 1 × 10^{-1} Torr at 123 K.

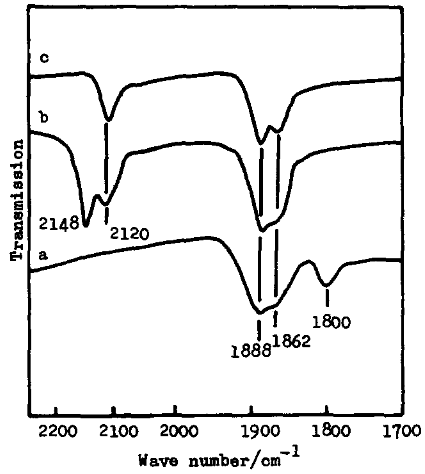

FIG. 8. IR differential spectra of alternate adsorption of NO and CO at 123 K. (a) 15 Torr NO adsorption, (b) 15 Torr CO adsorption after NO adsorption, (c) evacuated to 1 × 10^{-1} Torr at 123 K.

Al_2O_3 at 123 K. It shows three bands at 2170, 2148, and 2120 cm^{-1} (Fig. 7b). Then 15-Torr NO is introduced to the system at the same temperature, the band at 2170 cm^{-1} disappears, the band at 1888 cm^{-1} emerges with a shoulder at 1862 cm^{-1}, (Fig. 7c). After evacuation at 123 K, the band at 2148 cm^{-1} disappears (Fig. 7d). The results clearly indicate that preadsorbed CO on Cu^{2+} is replaced by NO adsorbed on Cu^{2+}.

The differential IR spectra of alternate adsorption in the reverse order are shown in Fig. 8. Preadsorption of 15-Torr NO presents three bands at 1888, 1862 (shoulder), and 1800 cm^{-1} at 123 K (Fig. 8a). When 15 Torr CO is introduced to the system at 123 K, the band at 1800 cm^{-1} disappears and CO adsorption on Cu^+ (2120 cm^{-1}) and CO physical adsorption (2148 cm^{-1}) are detected (Fig. 8b). After evacuation, only CO adsorption on Cu^+ and NO adsorption on Cu^{2+} sites exist. In this case, the species of CO adsorption replaces the species of NO adsorption on Cu^+ sites because CO adsorption is stronger than NO adsorption on Cu^+.

3.4. Coadsorption of CO and NO. Coadsorption of mixed gas of 15-Torr CO and 15-Torr NO gives almost the same result as that of alternate adsorption. After coadsorption for 5 min and evacuation at 123 K, IR spectrum shows three bands at 2125, 1888, and 1862 cm^{-1} (Fig. 9b). This is almost the same as Fig. 8c. The only difference is that the band of CO adsorption on Cu^+ sites is slightly shifted from 2120 to 2125 cm^{-1}.

All results of alternate adsorption and coadsorption explicitly show that when CO and NO coexist in the gas phase, CO is adsorbed on Cu^+ sites and NO is adsorbed on Cu^{2+} sites selectively.

DISCUSSION

Although the CuO/γ-Al_2O_3 sample is oxidized repeatedly and the bulk phase is composed of CuO and $CuAl_2O_4$, Cu^{2+} and Cu^+ coexist on the surface. Busca found a similar phenomenon on an unreduced CuO sample (*5*). Fierro and DeLa Bana (*14*) reported that the enthalpy of CuO formation (H_f^0) was the smallest and the amount of oxygen desorbed at 833 K was the largest among CuO, Co_3O_4, NiO, Fe_2O_3, SnO_2, Cr_2O_3, ZnO_2, TiO_2, Al_2O_3, and SiO_2. It probably reflects that CuO is the most unstable. During evacuation of the oxidized sample at room temperature, some oxygen vacancies are produced and Cu^{2+} ions are partially reduced to Cu^+.

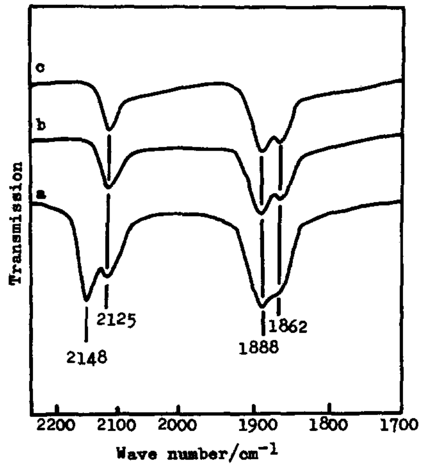

FIG. 9. IR differential spectra of CO and NO coadsorption on CuO/γ-Al_2O_3. (a) 123 K, (b) evacuated to 1 × 10^{-1} Torr at 123 K (c) 173 K.

TABLE 1

The Wavenumbers of IR Band, Adsorption Centers, the Relative Adsorption Strength, and Electron Configuration of CO and NO Adsorption

Adsorption T(K)	Probe molecule	Band (cm^{-1})	Adsorption center	Electron effect
123	CO	2170(w)	Cu^{2+}	M^--CO^+
		2120(s)	Cu^+	M^+-CO^-
	NO	1888(s)	$Cu^{2+}(CuO)$	M^--NO^+
		1862(m)	$Cu^{2+}(CuAl_2O_4)$	M : NO
		1800(w)	Cu^+	M^+-NO^-
	NO + CO	2125(s)	Cu^+	M^+-CO^-
		1888(S)	$Cu^{2+}(CuO)$	M^--NO^+
		1862(m)	$Cu^{2+}(CuAl_2O_4)$	M : NO
173	CO	2120(s)	Cu^+	M^+-CO^-
	NO	1888(s)	$Cu^{2+}(CuO)$	M^--NO^+
		1862(m)	$Cu^{2+}(CuAl_2O_4)$	M : NO

Note. s, strong; w, weak; m, middle.

The experimental results indicate that the two kinds of adsorption sites (Cu^{2+} and Cu^+) show a remarkable difference for probe molecular adsorption. Why do they exhibit such a different adsorption behavior and why is the selective adsorption present with both CO and NO? This may be explained by their electronic structure.

When the probe molecule (CO or NO) is adsorbed on the surface of the catalyst, there are two kinds of electronic interaction. One is the electronic donation from the probe molecule (σ-electron for CO or π^*-electron for NO) to empty *d*-orbital of the copper cation. The effect is strengthening of C–O bond for CO (or N–O bond for NO), then ν_{C-O} (or ν_{N-O}) shifts to higher frequency. The other one is the back-donation of the *d*-electron from the copper cation to an antibonding orbital of CO (or NO), the effect is weakening of the C–O bond for CO (or N–O bond for NO), and ν_{C-O} (or ν_{N-O}) shifts to lower frequency.

When CO is adsorbed on Cu^{2+} sites, the electron is mainly transferred from σ-orbital of CO to the *d*-orbital (d^9) of Cu^{2+}. When CO is adsorbed on Cu^+, the *d*-electron is donated from the *d*-orbital (d^{10}) of Cu^+ to π^*-orbital of CO. The σ-orbital energy of CO is lower than that of oxygen and carbon atoms, and it is rather stable. Therefore, it is difficult to transfer the σ-electron of CO. On the other hand, Cu^+ has one more electron than Cu^{2+} ion and the *d*-electron of Cu^+ is easier to donate from the 3*d*-orbital to the CO molecule than to that of Cu^{2+}. So CO adsorption on Cu^+ is stronger than adsorption on Cu^{2+}.

The electron is transferred from π^*-orbital of NO to 3*d*-orbital of Cu^{2+} during NO adsorption on Cu^{2+}. The reverse direction of electron transference appears for NO adsorption on Cu^+. As is known, the antibonding π^*-orbital of the NO molecule possesses one electron. The orbital energy is higher than that of oxygen and nitrogen atoms and the orbital is unstable. The π^*-electron is easy to transfer and the π^*-orbital is difficult to receive electron. So the NO adsorption on Cu^{2+} is stronger than that on Cu^+.

During coexistence of CO and NO on the CuO/γ-Al_2O_3 surface, competitive adsorption takes place. The weak adsorption is replaced by the strong one; that is, the selective adsorption takes place.

The difference between the NO vibration frequency of two kinds of Cu^{2+} (in CuO and in $CuAl_2O_4$) may originate from different a crystalline field. Further study of this is necessary.

CONCLUSION

In the oxidized CuO/γ-Al_2O_3 catalyst sample calcined at 1073 K, the bulk phase is composed of CuO and $CuAl_2O_4$, but Cu^{2+} and Cu^+ ions coexist on the surface. The wavenumbers of the IR bands, the adsorption centers, the relative adsorption strength, and the electron configuration of surface NO and CO at low temperatures are listed in Table 1. It was found that a selective chemisorption of CO/Cu^+ and NO/Cu^{2+} was formed when CO and NO coexisted in gas phase.

ACKNOWLEDGMENT

The support of the National Natural Science Foundation of China is gratefully acknowledged.

REFERENCES

1. Shelef, M., Otto, K., and Gandhi, H. S., *J. Catal.* **12,** 316 (1968).
2. Dictor, R., *J. Catal.* **109,** 89 (1988).
3. London, J. W., and Bell, A. T., *J. Catal.* **31,** 32 and 96 (1973).
4. Gandhi, H. S., and Shelef, M., *J. Catal.* **28,** 1 (1973).
5. Busca, G., *J. Mol. Catal.* **43,** 225 (1987).
6. Lokhov, Y. A., and Davydov, A. A., *Kinet. Catal.* **20,** 1018 and 1239 (1980).
7. Harrison, P. G., and Thornton, E. W., *J. Chem. Soc. Faraday Trans. 1* **74,** 2703 (1978).
8. Strohmeier, B. R., Leyden, D. E., Field, R. S., and Hercules, D. M., *J. Catal.* **94,** 514 (1985).
9. Castro, V. Di, Furtani, C., Gargano, M., and Rossi, M., *Appl. Surf. Sci.* **28,** 270 (1987).
10. Yin, L., Adler, I., Tsang, T., Matiengo, L., and Grims, O., *Chem. Phys. Lett.* **24,** 81 (1974).
11. Scrocco, M., *Chem. Phys. Lett.* **63,** 52 (1979).
12. Frost, D. C., Ishitani, A., and Mcdowell, C. A., *Mol. Phys.* **24,** 861 (1972).
13. Fu, Y. L., and Tian Y. C., *Chin. Chem. Soc.* **4,** 51 (1989).
14. Fierro, J. L. G., and De La Bana, J. F., *Catal. Rev.* **28,** 265 (1986).
15. Zaki, M. I., Vielhaber, B., and Knoezinger, H., *J. Phys. Chem.* **90,** 3176 (1986).